# Effect of an error field on the stability of the resistive wall mode

Richard Fitzpatrick

Citation: Physics of Plasmas (1994-present) **14**, 022505 (2007); doi: 10.1063/1.2446041
View online: http://dx.doi.org/10.1063/1.2446041
View Table of Contents: http://scitation.aip.org/content/aip/journal/pop/14/2?ver=pdfcov
Published by the AIP Publishing

# Effect of an error field on the stability of the resistive wall mode

Richard Fitzpatrick
*Institute for Fusion Studies, Department of Physics, University of Texas at Austin, Austin, Texas 78712*

(Received 26 October 2006; accepted 10 January 2007; published online 20 February 2007)

A simple model of the resistive wall mode (RWM) in a rotating tokamak plasma subject to a static error field is constructed, and then used to investigate RWM stability in a DIII-D–like [J. L. Luxon, Nucl. Fusion **42**, 614 (2002)] plasma. An error field as small as 10 G (i.e., about $5\times10^{-4}$ of the toroidal field) is found to significantly increase the critical plasma rotation frequency needed to stabilize the RWM. Such an error field also profoundly changes the nature of the RWM onset. At small error-field amplitudes, the RWM switches on gradually as the plasma rotation is gradually reduced. On the other hand, at large error-field amplitudes, there is a sudden collapse of the plasma rotation as the rotation frequency falls below some critical value. This collapse is associated with a very rapid switch-on of the RWM. © *2007 American Institute of Physics*.
[DOI: 10.1063/1.2446041]

## I. INTRODUCTION

The promising "advanced tokamak" (AT) concept is only economically attractive provided that the ideal external-kink $\beta$-limit is raised substantially due to the presence of a close-fitting electrically conducting wall.[2–4] (Here, $\beta=2\mu_0\langle p\rangle/B^2$, where $p$ is the plasma pressure, $B$ is the on-axis toroidal magnetic field strength, and $\langle\,\rangle$ denotes a volume average.) This, in turn, is only possible provided that the so-called *resistive wall mode* (RWM) is somehow stabilized.[5] Various tokamak experiments have established that the RWM can be stabilized by means of *plasma rotation*.[6–10] According to conventional theory, this stabilization is a combined effect of plasma *rotational inertia* and plasma *dissipation*.[11,12]

An "error field" is a small static asymmetry in the equilibrium magnetic field, **B**, of a tokamak. A given helical harmonic of an error field, of wave number **k**, is said to be *resonant* if $\mathbf{k}\cdot\mathbf{B}=0$ on some magnetic flux surface lying within the plasma. Likewise, a harmonic is said to be *near-resonant* if $\mathbf{k}\cdot\mathbf{B}=0$ on some flux surface lying just outside the plasma.

Now, a RWM is a plasma instability associated with a near-resonant magnetic perturbation. Not surprisingly, therefore, the near-resonant harmonics of an error field are strongly *amplified* by a tokamak plasma which is close to marginal stability for the RWM.[13] The near-resonant error-field harmonics also generate an *electromagnetic braking torque*. Such a torque reduces the plasma rotation, thereby bringing the RWM closer to marginal stability, thereby increasing the error-field amplification, thereby increasing the braking torque, etc.[14,15] Clearly, if the near-resonant harmonics of an error field are sufficiently large, then they can trigger a catastrophic collapse in the plasma rotation. Such a collapse is inevitably followed by the growth of the RWM.

All tokamaks possess intrinsic error fields which are the result of field-coil misalignments, uncompensated coil feeds, etc. Most are also equipped with *error-field correction coils* which allow the intrinsic error field to be partially cancelled out.[16] Using such coils to minimize the near-resonant harmonics of the error field, and thereby preventing any error-field triggered collapses of the plasma rotation, experimentalists have been able to significantly enhance the stability of AT discharges to the RWM.[17]

The aim of this paper is to examine the influence of a near-resonant error field on RWM stability in a DIII-D–like[1] tokamak. To achieve this goal, we shall employ a simple model of the RWM in which the free energy for the ideal external-kink mode is derived from plasma current gradients, rather than pressure gradients, and the plasma dissipation is provided by *neoclassical flow damping*.[19]

## II. RWM MODEL

### A. Plasma response to a RWM

Consider a large aspect-ratio, low-$\beta$, circular cross-section tokamak plasma of major radius $R_0$, minor radius $a$, on-axis toroidal magnetic field strength $B_0$, and on-axis plasma mass density $\rho_0$. The *inverse aspect ratio* of the plasma is $\epsilon_0=a/R_0$.

In the following, all lengths are normalized to $a$, all magnetic field strengths to $B_0$, all mass densities to $\rho_0$, and all times to the hydromagnetic time scale $\tau_H=(R_0/B_0)\sqrt{\mu_0\rho_0}$.

The plasma equilibrium is described by the model safety-factor profile

$$q(r)\equiv\frac{r\epsilon_0}{B_\theta(r)}=\frac{q_a r^2}{1-(1-r^2)^{q_a/q_0}},\tag{1}$$

and the model density profile

$$\rho(r)=(1-r^2)^\alpha.\tag{2}$$

Here, $r$ is the radial distance from the magnetic axis, $q_a$ is the safety factor at the edge of the plasma, and $q_0$ is the safety factor on the magnetic axis.

The plasma response to the near-resonant helical magnetic perturbation generated by a RWM (with, say, $m$ periods in the poloidal direction, and $n$ periods in the toroidal direction) is governed by the eigenmode equation[19,20]

 

$$r\frac{d}{dr}\left[\left(\rho\gamma'^2\left[1+\frac{q^2}{\epsilon_0^2}\frac{\mu_\parallel}{\gamma'+\mu_\parallel r^2}\right]+Q^2\right)r\frac{d\phi}{dr}\right] - \left[m^2\left(\rho\gamma'\left[\gamma'+\frac{q^2}{\epsilon_0^2}\mu_\parallel\right]+Q^2\right)+r\frac{dQ^2}{dr}\right]\phi\simeq 0, \tag{3}$$

where $\gamma'=\gamma-\mathrm{i}(m\Omega_\theta-n\Omega_\phi)$ is the mode growth rate in the plasma frame, $\gamma$ is the growth rate in the laboratory frame, $\Omega_\theta$ is the plasma poloidal angular rotation velocity, and $\Omega_\phi$ is the plasma toroidal angular rotation velocity. Note that $m\Omega_\theta-n\Omega_\phi$ is assumed to be *uniform* across the plasma in this paper, for the sake of simplicity. Furthermore, $Q(r)=m/q(r)-n$, and $-\gamma'\phi$ is the perturbed scalar electric potential associated with the instability. Finally,

$$\mu_\parallel=\frac{3}{2}\frac{\epsilon_0^4}{q^2}\frac{\eta_0}{\rho} \tag{4}$$

is the *neoclassical parallel ion viscosity*. Here, $\eta_0$ is the parallel ion viscosity specified in Ref. 21.

As is well known, expression (4) is only valid in a highly collisional plasma. However, following Ref. 22, we can obtain a more general expression, which is valid over a wide range of plasma collisionalities, by writing

$$\mu_\parallel=\frac{3}{2}\frac{\epsilon_0^4}{q^2}\frac{\eta_0}{\rho}F(\nu_*), \tag{5}$$

where

$$F(\nu_*)=\frac{\nu_*}{(3.23\epsilon^{3/2}+3.15\epsilon^{3/4}\nu_*^{1/2}+\nu_*)}\frac{\nu_*}{(1.52+\nu_*)} \tag{6}$$

and

$$\nu_*=\frac{q}{\epsilon v_i\tau_i}. \tag{7}$$

Here, $\epsilon=r/R_0$, $v_i$ is the ion thermal velocity, and $\tau_i$ is the ion collision time specified in Ref. 21. Thus, $\nu_*\gg 1$ corresponds to the highly collisional *Pfirsch-Schlüter* regime, $\nu_*\sim 1$ to the intermediate *plateau* regime, and $\nu_*\ll\epsilon^{3/2}$ to the weakly collisional *banana* regime.[23]

Finally, launching a well-behaved solution to Eq. (3) from the magnetic axis ($r=0$), and integrating to the edge of the plasma ($r=1$), we obtain the complex *plasma response parameter*

$$s=-\frac{1}{2}\left[1+m^{-1}\frac{d\ln(Q\phi)}{d\ln r}\right]_{r=1}. \tag{8}$$

This parameter *fully specifies* the response of the plasma to the RWM.

### B. RWM dispersion relation

Suppose that the plasma is surrounded by a thin resistive wall. By matching the plasma and vacuum solutions at the edge of the plasma, it is a relatively straightforward task to obtain the (single mode) *RWM dispersion relation*:[24]

$$\gamma[c-(1-c)s]-\gamma_w s=0. \tag{9}$$

Here, $0<c<1$ is a dimensionless parameter which determines the degree of coupling between the plasma and the wall, whereas $\gamma_w$ is the characteristic rate at which an $m$, $n$ magnetic field diffuses through the wall. The above dispersion relation can easily be solved numerically, via Newton iteration, to obtain the RWM growth rate, $\gamma$.

### C. Plasma stability parameter

The *marginally stable ideal eigenmode equation*,

$$r\frac{d}{dr}\left(Q^2r\frac{d\phi}{dr}\right)-\left(m^2Q^2+r\frac{dQ^2}{dr}\right)\phi\simeq 0, \tag{10}$$

is obtained from Eq. (3) by neglecting plasma inertia, and governs the stability of the ideal external-kink mode.[25] Calculating the plasma response parameter (8) from the above equation, we obtain a *real* number, $s_b$, which is equivalent to the well-known Boozer stability parameter for the ideal external-kink mode.[24] It can be demonstrated that the $m$, $n$ ideal external-kink mode is unstable when the wall is absent provided that $s_b>0$, and is unstable even if the wall is perfectly conducting provided that $s_b>s_c\equiv c/(1-c)$.[24,25] Hence, we can define a real *plasma stability parameter*:

$$\bar{s}=\frac{s_b}{s_c}. \tag{11}$$

The so-called *no-wall stability limit* corresponds to $\bar{s}=0$, whereas the *perfect-wall stability limit* corresponds to $\bar{s}=1$.

### D. Plasma response to an error field

Suppose that the plasma is subject to a near-resonant static error field with the same helicity as the RWM, i.e., $m$ periods in the poloidal direction, and $n$ periods in the toroidal direction. Such an error field does not directly influence the stability of the RWM (because of the frequency mismatch between the RWM and the error field), but does indirectly influence RWM stability by *braking* the plasma rotation. We can determine the response of the plasma to the error field by using Eq. (3) (with $\gamma=0$) to calculate an analogous plasma response parameter to that defined in Eq. (8) for the RWM. Let us call this complex error-field response parameter $s'$. The interpretation of $s'$ is very straightforward. If $b_r$ is the radial component of the error field at $r=1$ in the absence of a plasma, then in the presence of the plasma the radial error field at $r=1$ is $b_r/(-s')$.[13] Hence, $s'$ parameterizes the *amplification* of the error field by the plasma.

The net poloidal and toroidal electromagnetic torques exerted on the plasma by the error field are[14]

$$T_\theta=-\frac{4\pi^2}{\epsilon_0}\frac{n}{m}\frac{\mathrm{Im}(s')}{|s'|^2}b_r^2, \tag{12}$$

$$T_\phi=\frac{4\pi^2}{\epsilon_0}\frac{\mathrm{Im}(s')}{|s'|^2}b_r^2, \tag{13}$$

respectively.

Now, we can write the poloidal and toroidal equations of motion of the plasma in the form

$$I_\theta\left[\frac{d\Omega_\theta}{dt}+(\Omega_\theta-\Omega_\theta^{(0)})(\tau_\theta^{-1}+\tau_M^{-1})\right]=T_\theta, \tag{14}$$

$$I_\phi\left[\frac{d\Omega_\phi}{dt}+(\Omega_\phi-\Omega_\phi^{(0)})\tau_M^{-1}\right]=T_\phi, \tag{15}$$

respectively. Here,

$$I_\theta=\frac{2\pi^2}{\epsilon_0}\frac{1}{(1+\alpha)(2+\alpha)}, \tag{16}$$

$$I_\phi=\frac{2\pi^2}{\epsilon_0^3}\frac{1}{(1+\alpha)} \tag{17}$$

are the poloidal and toroidal moments of inertia of the plasma, respectively, $\tau_M$ is the *toroidal momentum confinement time*, and

$$\tau_\theta^{-1}=\left\langle\frac{q^2}{\epsilon_0^2}\mu_\parallel\right\rangle \tag{18}$$

is the *neoclassical poloidal flow-damping time*. Here, $\langle\cdots\rangle$ denotes an average over the plasma volume. Finally, $\Omega_\theta^{(0)}$ and $\Omega_\phi^{(0)}$ are the poloidal and toroidal angular velocities of the plasma, respectively, in the *absence* of the error field.

The angular frequency of the RWM is

$$\Omega=m\Omega_\theta-n\Omega_\phi. \tag{19}$$

Let $\Omega^{(0)}$ be the corresponding frequency in the absence of an error field. It follows, from the above equations, that in a *steady state*

$$\Omega^{(0)}=\Omega+G\frac{\mathrm{Im}(s')}{|s'|^2}b_r^2, \tag{20}$$

where

$$G=2(1+\alpha)\left[m\frac{(2+\alpha)}{\tau_\theta^{-1}+\tau_M^{-1}}+\frac{n^2}{m}\frac{\epsilon_0^2}{\tau_M^{-1}}\right]. \tag{21}$$

Note that $\Omega\leq\Omega^{(0)}$ in Eq. (20), since $\mathrm{Im}(s')>0$ and $G>0$. Hence, the error field *brakes* the plasma rotation. Furthermore, the above steady-state solution is only dynamically stable provided that $d\Omega^{(0)}/d\Omega>0$. [Both $\Omega$ and $\Omega^{(0)}$ are assumed to be uniform across the plasma, for the sake of simplicity.]

### E. Error-field induced bifurcations in Ω

Figure 1 shows a typical $\Omega^{(0)}$ versus $\Omega$ curve. In this particular case, there is a *forbidden band*[14,26,27] of mode rotation frequencies in which there are no stable solutions of the steady-state force-balance equation (20) [since $d\Omega^{(0)}/d\Omega<0$]. Hence, the steady-state mode frequency $\Omega$ cannot lie in this band. Instead, when $\Omega$ reaches either the upper or lower boundaries of the forbidden band there is a *bifurcation* to a solution on the opposite side of the band (see Fig. 1). Such a bifurcation is accompanied by a sudden reduction or increase, respectively, in $\Omega$.[14,26,27] In general, there is considerable *hysteresis* in this process.

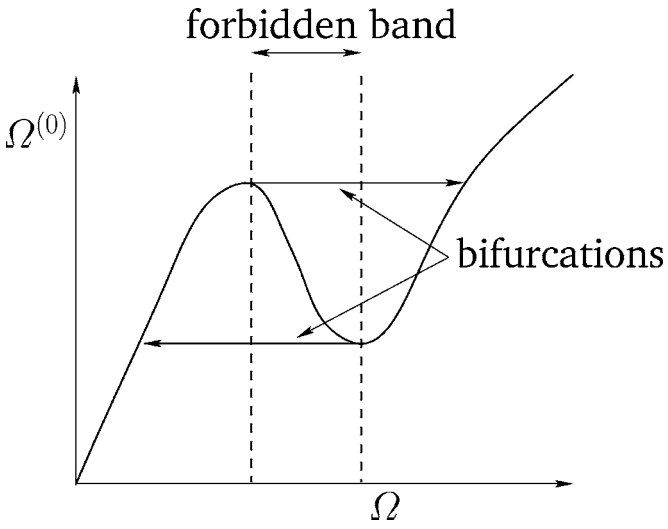


FIG. 1. Typical $\Omega^{(0)}$ versus $\Omega$ curve.

### F. Summary

We have outlined a simple model of the RWM in a rotating tokamak plasma. This model contains sufficient physics to allow us to investigate the effect of a near-resonant error field on RWM stability in a DIII-D-like plasma. The plasma dissipation in our model is provided by neoclassical flow damping. Such dissipation is strongly peaked at the edge of the plasma. Hence, it is a reasonable approximation to replace the neoclassical viscosity (5) and the volume averaged flow-damping rate (18) by values calculated at the *edge* of the plasma.

## III. THE DIII-D TOKAMAK

### A. Plasma parameters

The DIII-D tokamak[1] has a major radius $R_0=1.69$ m, minor radius $a=0.61$ m, typical on-axis toroidal field strength $B_0=2.1$ T, and typical on-axis electron number density $n_0=6\times10^{19}$ m$^{-3}$.[18] It follows that $\tau_H=3\times10^{-7}$ s. The typical toroidal momentum confinement time is $\tau_M=60$ ms, giving $\tau_M=2\times10^5$ in normalized units.[8]

The typical electron number density, electron temperature, and ion temperature at the edge of a DIII-D discharge are $n_e=2\times10^{19}$ m$^{-3}$, $T_e=100$ eV, and $T_i=100$ eV, respectively.[28] This implies that $\nu_*=0.82$, $\mu_\parallel=1\times10^{-4}$ and $\tau_\theta=1\times10^2$ in normalized units.

### B. Wall parameters

The DIII-D wall parameters, $c$ and $\gamma_w$, are determined by fitting to data obtained from the VALEN code.[29] VALEN, which calculates the RWM growth rate as a function of the Boozer stability parameter, $s_b$, for a dissipationless plasma, accurately models the DIII-D wall in three dimensions via a finite-element representation which uses a standard thin-shell integral formulation. The plasma is represented as a surface current.

Figure 2 shows the growth rate of a predominately 3, 1 RWM versus the Boozer stability parameter, calculated by

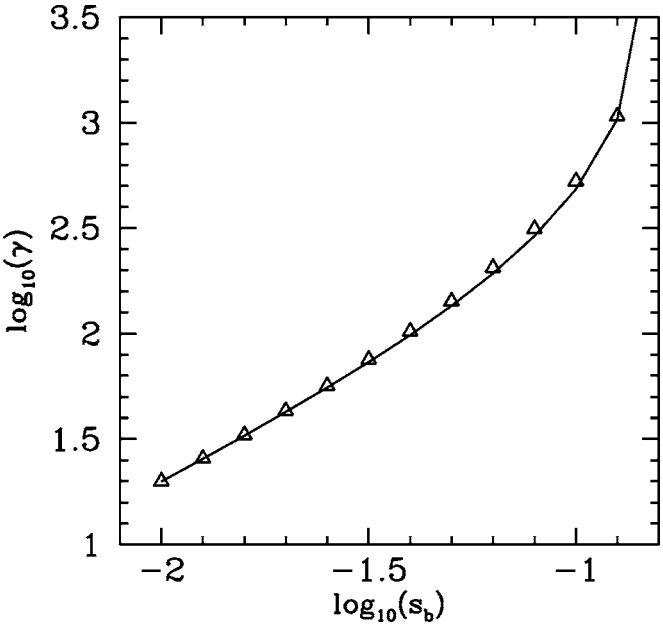


FIG. 2. The points show the growth rate of a predominately 3, 1 RWM (in inverse seconds) versus the Boozer stability parameter, calculated by VALEN for DIII-D discharge 92544. The curve shows the fit of the single-mode RWM dispersion relation (9) to these data.

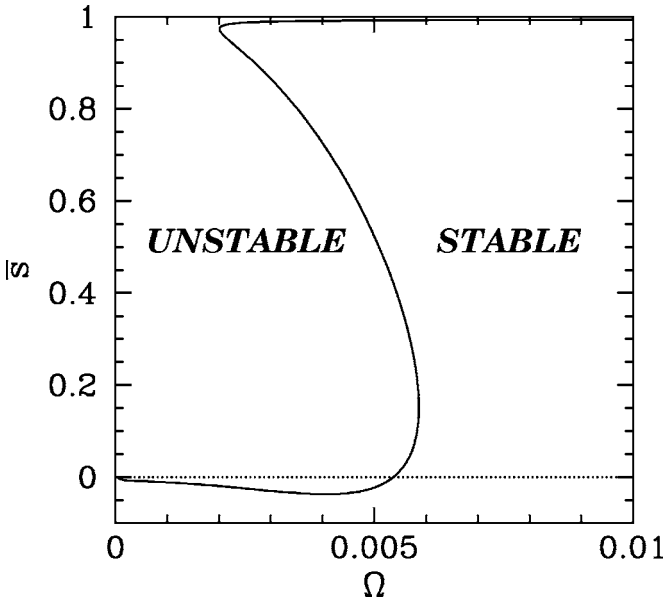


FIG. 3. RWM stability boundary in the absence of an error field plotted in the normalized plasma rotation versus plasma stability space. The calculation parameters are $m=3$, $n=1$, $\alpha=0.5$, $q_a=2.95$, $\epsilon_0=0.36$, $\mu_\parallel=1\times10^{-4}$, $c=0.14$, and $\gamma_w=8\times10^{-5}$. The no-wall and perfect-wall stability boundaries lie at $\bar{s}=0$ and $\bar{s}=1$, respectively.

VALEN for a typical DIII-D RWM discharge. Also shown is the best fit of the single-mode RWM dispersion relation (9) to these data. The fitting parameters are $c=0.14$ and $\gamma_w=262\ \mathrm{s}^{-1}$. In normalized units, $\gamma_w=8\times10^{-5}$. It can be seen that the fit to the data is fairly good.

## IV. NUMERICAL RESULTS

### A. Introduction

The RWM model outlined in Sec. II has been implemented numerically. In the following, we shall discuss some of the predictions of this model obtained using the estimated DIII-D plasma and wall parameters given in Sec. III.

### B. RWM stability boundary

Figure 3 shows the 3, 1 RWM stability boundary predicted by the model, plotted in plasma rotation versus plasma stability space. The plasma stability is varied by changing $q_0$, while keeping $q_a$ fixed. According to the figure, the RWM is completely stabilized, allowing the plasma to reach the perfect-wall stability boundary for the ideal external-kink mode, whenever the plasma rotation frequency exceeds about 0.6% of the hydromagnetic frequency, $\tau_H^{-1}$.

### C. Effect of error field on critical rotation frequency

Figures 4 and 5 illustrate the effect of a 3, 1 error field on the critical rotation frequency required to stabilize the 3, 1 RWM. Note that Fig. 5 shows a case where the plasma is closer to the perfect-wall stability limit than the plasma in Fig. 4, i.e., Fig. 5 shows a higher "effective $\beta$" plasma than Fig. 4. At small error-field amplitudes, as the plasma rotation frequency is gradually reduced, and falls below the critical rotation frequency calculated in the *absence* of the error field, the RWM passes smoothly through marginal stability, and there is a *gradual* onset of the mode. On the other hand, if the error-field amplitude is sufficiently large that the critical rotation frequency lies in the *forbidden band* of rotation frequencies (see Sec. II E) then, as the plasma rotation fre-

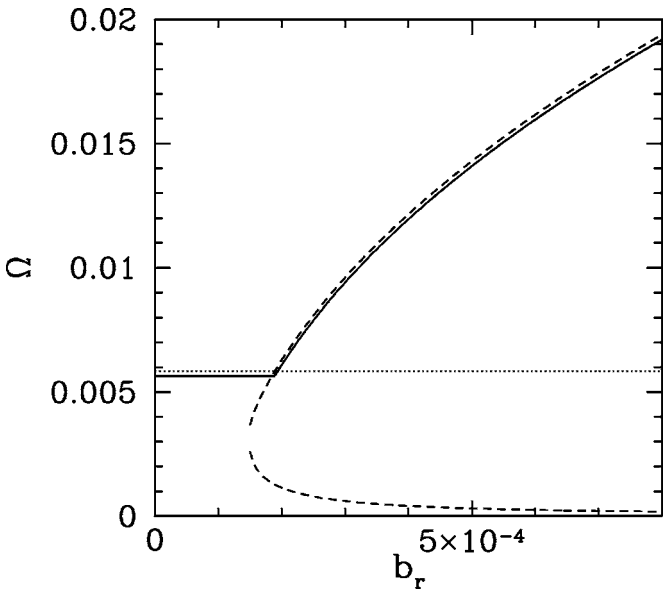


FIG. 4. RWM stability boundary in the presence of an error field of the same helicity plotted in the error-field strength versus normalized plasma rotation space. The calculation parameters are $m=3$, $n=1$, $\alpha=0.5$, $q_a=2.95$, $\bar{s}=0.2$, $\epsilon_0=0.36$, $\mu_\parallel=1\times10^{-4}$, $c=0.14$, and $\gamma_w=8\times10^{-5}$, $\tau_\theta=1\times10^2$, and $\tau_M=2\times10^5$. The horizontal dotted line shows the critical rotation rate for RWM stabilization in the absence of an error field. The upper and lower short-dashed curves show the forbidden band of plasma rotation rates. The solid curve (slightly displaced for the sake of clarity) shows the effective critical rotation rate for RWM stabilization in the presence of the error field.

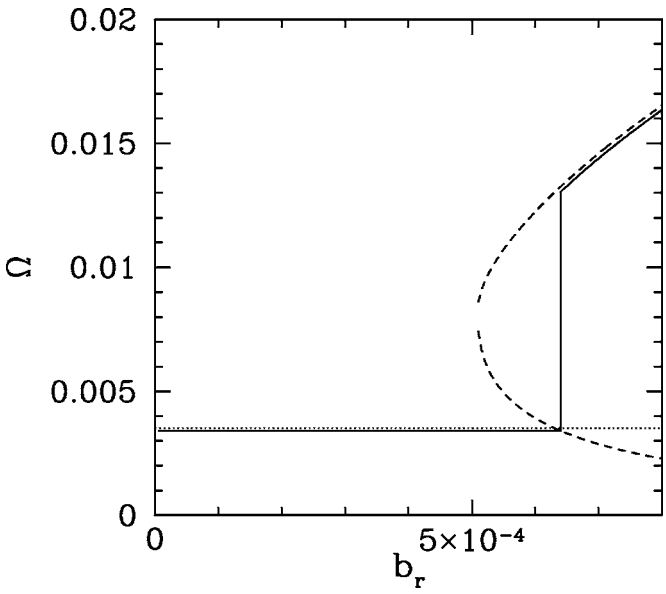


FIG. 5. RWM stability boundary in the presence of an error field of the same helicity plotted in error-field strength versus normalized plasma rotation space. The calculation parameters are $m=3$, $n=1$, $\alpha=0.5$, $q_a=2.95$, $\bar{s}=0.8$, $\epsilon_0=0.36$, $\mu_\parallel=1\times10^{-4}$, $c=0.14$, and $\gamma_w=8\times10^{-5}$, $\tau_\theta=1\times10^2$, and $\tau_M=2\times10^5$. The horizontal dotted line shows the critical rotation rate for RWM stabilization in the absence of an error field. The upper and lower short-dashed curves show the forbidden band of plasma rotation rates. The solid curve (slightly displaced for the sake of clarity) shows the effective critical rotation rate for RWM stabilization in the presence of the error field.

quency is gradually reduced, it enters the forbidden band, from above, while the RWM is still *stable*. At this point, the rotation frequency jumps from above to below the forbidden band, as discussed in Sec. II E, ending up at a value well below that needed to stabilize the RWM. In other words, there is a sudden collapse in the plasma rotation frequency, and virtually all of the rotation stabilization of the RWM is lost, rendering the RWM highly unstable.

It is clear, from Figs. 4 and 5, that a near-resonant error field profoundly changes the manner in which the RWM switches on as the plasma rotation frequency is gradually reduced. At low error-field amplitudes, the switch-on is *gradual*, whereas at high amplitudes the switch-on is *sudden*, and is associated with a *collapse* in the plasma rotation. It is also clear, from the figures, that a sufficiently large amplitude error field *increases* the effective critical rotation rate required to stabilize the RWM, which becomes the upper boundary of the forbidden band of rotation frequencies, rather than the rotation frequency at which the RWM is marginally stable.

Incidentally, a comparison of Figs. 4 and 5 suggests that a near-resonant error field has less and less effect on the RWM as the plasma moves closer and closer to the perfect-wall stability boundary.

Finally, from Fig. 4, it can be seen that an error field whose amplitude (measured as the vacuum $b_r$ at the edge of the plasma) is as low as $5\times10^{-4}\ B_0$ (i.e., about 10 G) can *triple* the effective critical rotation rate required to stabilize the RWM in a DIII-D-like plasma.

## V. SUMMARY

We have constructed a simple model of the RWM in a rotating tokamak plasma subject to a static error field. We have then used this model to investigate the effect of a near-resonant error field on RWM stability in a DIII-D–like plasma. We find that an error field as small as 10 G (i.e., about $5\times10^{-4}$ of the toroidal field) can *significantly increase* the critical plasma rotation frequency needed to stabilize the RWM. Such an error field also profoundly changes the nature of the RWM onset. In the absence of an error field, or at small error-field amplitudes, the RWM switches on *gradually* as the plasma rotation is gradually reduced. On the other hand, at large error-field amplitudes, there is a *sudden collapse* of the plasma rotation as the rotation frequency falls below some critical value. This collapse is associated with a very rapid switch-on of the RWM.

## ACKNOWLEDGMENTS

The author would like to thank Jim Bialek (Columbia University) for providing the VALEN data used in this paper. The author would also like to acknowledge helpful discussions with Andrea Garofalo (Columbia University), Ted Strait (General Atomics), and Michio Okabayashi (Princeton Plasma Physics Laboratory).

This research was funded by the U.S. Department of Energy under Contract No. DE-FG05-96ER-54346.

[1] J. L. Luxon, Nucl. Fusion **42**, 614 (2002).
[2] F. Troyon, R. Gruber, H. Saurenmann, S. Semenzato, and S. Succi, Plasma Phys. Controlled Fusion **26**, 209 (1984).
[3] C. Kessel, J. Manickam, G. Rewoldt, and W. M. Tang, Phys. Rev. Lett. **72**, 1212 (1994).
[4] E. A. Lazarus, G. A. Navratil, C. M. Greenfield *et al.*, Phys. Rev. Lett. **77**, 2714 (1996).
[5] J. P. Goedbloed, D. Pfirsch, and H. Tasso, Nucl. Fusion **12**, 649 (1972).
[6] M. Okabayashi, N. Pomphrey, J. Manikam *et al.*, Nucl. Fusion **36**, 1167 (1996).
[7] A. M. Garofalo, E. Eisner, T. H. Ivers *et al.*, Nucl. Fusion **38**, 1029 (1998).
[8] A. M. Garofalo, E. J. Strait, L. C. Johnson *et al.*, Phys. Rev. Lett. **89**, 235001 (2002).
[9] S. A. Sabbagh, J. M. Bialek, R. E. Bell *et al.*, Nucl. Fusion **44**, 560 (2004).
[10] M. Shilov, C. Cates, R. James *et al.*, Phys. Plasmas **11**, 2573 (2004).
[11] A. Bondeson and D. J. Ward, Phys. Rev. Lett. **72**, 2709 (1994).
[12] R. Betti and J. P. Freidberg, Phys. Rev. Lett. **74**, 2949 (1995).
[13] A. H. Boozer, Phys. Rev. Lett. **86**, 5059 (2001).
[14] R. Fitzpatrick, Nucl. Fusion **33**, 1049 (1993).
[15] R. Fitzpatrick, Phys. Plasmas **9**, 3459 (2002).
[16] J. T. Scoville and R. J. La Haye, Nucl. Fusion **43**, 250 (2003).
[17] E. J. Strait, J. M. Bialek, I. N. Bogatu *et al.*, Phys. Plasmas **11**, 2505 (2004).
[18] H. Remeerdes, T. C. Hender, S. A. Sabbagh *et al.*, Phys. Plasmas **13**, 056107 (2006).
[19] R. Fitzpatrick, Phys. Plasmas **13**, 072512 (2006).
[20] K. C. Shaing, Phys. Plasmas **11**, 5525 (2004).
[21] S.I. Braginskii, "Transport processes in a plasma," in *Reviews of Plasma Physics* (Consultants Bureau, New York, 1965), Vol. 1, p. 205.
[22] J. D. Callen, W. X. Qu, K. D. Siebert, B. A. Carreras, K. C. Shaing, and D. A. Spong, in *Plasma Physics and Controlled Nuclear Fusion Research 1986*, Proceedings of the 11th International Conference (International Atomic Energy Agency, Vienna, 1987), Vol. 2, p. 157.

[23]J. Wesson, *Tokamaks*, 3rd ed. (Oxford University Press, Oxford, 2004).
[24]A. H. Boozer, Phys. Plasmas **5**, 3350 (1998).
[25]W. A. Newcomb, Ann. Phys. (N.Y.) **10**, 232 (1960).
[26]D. A. Gates and T. C. Hender, Nucl. Fusion **36**, 273 (1996).
[27]C. G. Gimblett and R. J. Hastie, Phys. Plasmas **11**, 1019 (2004).
[28]W. M. Stacey and R. J. Groebner, Phys. Plasmas **13**, 012513 (2006).
[29]J. Bialek, A. H. Boozer, M. E. Mauel, and G. A. Navratil, Phys. Plasmas **8**, 2170 (2001).